scientific reports

Check for updates

OPEN

Trophoblast cell-derived extracellular vesicles regulate the polarization of decidual macrophages by carrying miR-141-3p in the pathogenesis of preeclampsia

Dongcai Wu[1,6], Bo Zhou[2,6], Lan Hong[3], Hui Cen[1], Ling Wang[1], Yanlin Ma[4] & Humin Gong[5]✉

Dysregulation of macrophage polarization can prevent the invasion of trophoblast cells and further limit spiral artery remodeling in preeclampsia (PE). However, its mechanism is obscure. HTR8-/Svneo cells were cultured under normoxic or hypoxic conditions and extracellular vesicles (EVs) in the culture supernatants were extracted. Next, the cells were incubated with those EVs to investigate their effects on trophoblasts. A co-culture system consisting of HTR8-/Svneo cells and macrophages was used to reveal how the trophoblast-derived EVs affected the macrophage subtype. Finally, a PE mouse model and miR-141-3p knockout mice were used to verify the function of miR-141-3p in PE. Hypoxia induced abnormal increases in the levels of miR-141-3p in HTR8-/Svneo cells and EVs. EVs from hypoxia-treated HTR8-/Svneo cells could downregulate PTEN, a potential target of miR-141-3p, and inhibit trophoblast mitophagy and invasion. However, HTR8-/Svneo cells transfected with an miR-141-3p inhibitor could attenuate the influence of EVs. In an HTR8-/Svneo cell plus macrophage co-culture system, hypoxia-pretreated cells promoted the transformation of macrophages into the M1-phenotye, and HTR8-/Svneo invasion was inhibited by the macrophages. MiR-141 from EVs could target and downregulate dual specificity phosphatase 1 (DUSP1) expression in macrophages, induce formation of the M1 macrophage phenotype in THP-1 cells, downregulate DUSP1 expression, and upregulate TAB2/TAK1 signaling. These results were also demonstrated in normal pregnant mice and PE pregnant mice. A hypoxic environment could upregulate miR-141 expression in the EVs of HTR8-/Svneo cells, and THP-1-derived macrophages could uptake EVs releasing miR-141 to downregulate DUSP1 expression and induce the formation of M1 macrophages, which can lead to the development of PE.

Keywords Exosome, Macrophage, Trophoblast, Angiogenesis, Preeclampsia

Background

Preeclampsia (PE) is a placental disease that presents with hypertension and involves multiple system disorder during pregnancy. It is a main cause of maternal, fetal, and neonatal morbidity and mortality, especially in

[1]Department of Obstetrics, Hainan General Hospital, Hainan Affiliated Hospital of Hainan Medical University, Haikou, China. [2]Hainan Medical University, Haikou, China. [3]Department of Gynecology, Hainan General Hospital, Hainan Affiliated Hospital of Hainan Medical University, Haikou, China. [4]Hainan Provincial Key Laboratory for human reproductive medicine and Genetic Research & Hainan Provincial Clinical Research Center for Thalassemia & Key Laboratory of Reproductive Health Diseases Research and Translation, Ministry of Education, The First Affiliated Hospital of Hainan Medical University, Hainan Medical University, Haikou, China. [5]Department of Obstetrics, Hainan Affiliated Hospital of Hainan Medical University, Hainan General Hospital, Haikou, China. [6]Dongcai Wu and Bo Zhou contributed equally to this article. ✉email: gonghm163@163.com

developing regions and countries. Worse still, there are no curative treatments except for termination of pregnancy[1].

Cytotrophoblasts are major components of the placenta. In early pregnancy, they can differentiate into extravillous trophoblasts (EVTs), some of which infiltrate into the deep layer of endometrium and become interstitial trophoblast cells, while others invade the spiral arteries in maternal decidua and uterine myometrium. The invading EVTs gradually replace vascular endothelial cells and become vascular trophoblast cells. This remodeling process transforms the spiral artery from a high resistance vessel to a volume vessel, meeting the blood oxygen and nutrition needs of the placenta[2]. However, the invasion of EVTs is inadequate in pregnant women with PE, leading to placental hypoxia and ischemia, and further fetal growth restriction. On the other hand, the inflammatory factors secreted by trophoblast cells can impair the function of vascular endothelium, induce an excessive inflammatory response, and further enhance the development of preeclampsia[3]. Therefore, EVT invasion is indispensable for placentation and pregnancy.

MicroRNAs (miRNA), a category of small noncoding RNAs, negatively regulate gene expression by targeting their mRNAs. The search for biomarkers of PE via genome-wide analysis has found that miRNAs function in the human placenta[4–6]. In human placental cells, miRNA profiles change during stages of pregnancy and reflect the development and health of gestation. MiRNAs are released by cells that secrete extracellular vesicles (EVs), such as exosomes. Exosomes can be identified and internalized by other cells to mediate intercellular communications. Report suggested that placental exosomes hold promise as a valuable avenue for deciphering the complexities of preeclampsia[7]. In addition, researchers found that the level of miR-222-3p and miR-199a-5p in plasma exosomes was elevated in PE patients and it influenced the proliferation, invasion and migration of HTR-8/Svneo cells[8,9]. Recent literature reported miR-27a and miR-92a could regulate macrophage phenotype in preeclamptic placenta[10,11]. Therefore, it was speculated that trophoblast-derived EVs are capable of targeting immune cells. A previous study revealed communications that occur between trophoblast cells and immune cells are involved with PE development[12].

The mononuclear phagocyte system (MPS) is an important component of the immune system, as it functions in the inflammatory response, immune regulation, and cell physiological regulation. At the beginning of pregnancy, monocytes infiltrate the decidua of the uterus and develop into decidual macrophages (DMs). In a normal pregnancy, DMs differentiate into M2-macrophages, which promote spiral remodeling, trophoblast fragment phagocytosis, and inflammation regulation, and are of great significance for maintaining maternal fetal tolerance. In the process of preeclampsia, DMs differentiate into M1-macrophages that produce inflammatory factors that lead to placental dysplasia[13]. Macrophage polarization is strongly correlated with PE development. M1-macrophages inhibit the transfer of trophoblastic cells, while M2-macrophages promote that transfer, suggesting that macrophage polarization affects the invasion of trophoblasts and the formation of spiral arteries[14]. However, whether trophoblasts affect macrophage polarization via EVs is not clear.

In PE placenta, researchers have found elevated levels of miRNA-141 which regulated trophoblast invasion[12]. Moreover, miRNA-141 in trophoblast-derived EVs can reduce the proliferation of allogeneic T cells. In previous study, we also found that miRNA-141-3p regulates trophoblast apoptosis, invasion, and vascularization by blocking CXCL12β/CXCR2/4 signal transduction under a hypoxic environment[15]. In the presented study, we found that the levels of exosome-derived miRNA-141-3p were increased in HTR8-/Svneo cells cultured under conditions of hypoxia, and those increased levels affected HTR8-/Svneo cells and THP-1-derived macrophages through autocrine or paracrine pathways, respectively.

Materials and methods

Cell culture

THP-1 cells and HTR-8/Svneo cells were provided by the American Type Culture Collection (ATCC, Manassas, VA, USA). Both cell lines were cultured in RPMI 1640 medium supplemented with 10% FBS and 1% penicillin-streptomycin-neomycin antibiotic mixture (Thermo Fisher Scientific, Waltham, MA, USA) at 37°C in an incubator under a mixture of 5% CO_2 and 95% air. To obtain macrophages, THP-1 cells were treated with PMA (100ng/mL, 48 h; MCE, Princeton, NJ, USA), and subsequently stimulated with IL-4 (6 h, 100 ng/mL; Solarbio, Beijing, China). To create a co-culture system, HTR-8/Svneo cells and macrophages were seeded into the lower chamber and upper chamber of a Transwell plate, respectively. To cultivate cells under conditions of hypoxia, an AraeroPack-MicroAero generator (Mitsubishi MGC, Japan) was used according to the manufacturer's instructions.

EVs isolation and scanning electron microscope detection

20 mL of Supernatant were collected by successive centrifugations and EVs were purified using Exosome Isolation Reagent (Ribo Bio, Guangzhou, China). The particle sizes and concentrations of EVs were measured using a NanoSight NS300 system (Malvern Panalytical, Shanghai, China), and their morphology was examined by transmission electron microscopy (TEM) (Olympus, Tokyo, Japan). TEM was also used for detecting cell morphology and intracellular autophagosomes. For co cultivation with cells, PKH26 labeled EVs (10^5 particles/1 ml) were added to macrophages (1×10^4) of HTR-8/Svneo cells (1×10^4).

Quantitative real-time polymerase chain reaction (qRT-PCR)

The total RNA was extracted from cells and trophoblast/ decidua tissues by using TRIzol reagent (Invitrogen, Carlsbad, CA, USA), and the miRNAs were extracted from EVs (10^5 particles/1 ml) by a MirVana ™ miRNA Separation Kit (Thermo Fisher Scientific). The reverse transcription was performed using a cDNA Synthesis Kit (TaKaRa, Tokyo, Japan), total RNA (1 μg) and primers that specifically targeted miRNA (Table S1). Next, the levels of miR-141-3p were detected by using SYBR Premix Ex Taq (TaKaRa) on an RT-PCR system. U6

and cel-miR-39 served as internal controls in cells and EVs, respectively. Synthetic cel-miR-39 (10nmol) was added to 1 mL medium containing 10^5 particles EVs. All PCR primers were chemo-synthesized by IGE Biotech (Guangzhou, China) and are shown in Table S1. PCR reaction process: 94 ℃ for 2 min, 94 ℃ for 20 s, 58 ℃ for 20 s, 72 ℃ for 20 s, 40 cycles. Relative gene transcription levels were calculated using the $2^{-\Delta\Delta CT}$ method.

Cell activity detection

Cell counting kit-8 (CCK-8, Beyotime, Shanghai, China) assays were performed to quantify cellular activity. Briefly, after group processing, the cells (1×10^4) were harvested and seeded into a culture plate; after which, they were incubated with CCK-8 solution (10 μL per well) at 37 °C for 4 h. Finally, the optical density (OD) of each well at a wavelength of 450 nm was detected with a microplate reader (Thermo Fisher Scientific).

Western blotting

Cells (1×10^6) or tissue samples were milled and their total proteins were extracted with RIPA lysis buffer. Samples of protein were separated by electrophoresis, and the protein bands were transferred onto PVDF membranes, which were subsequently incubated with primary antibodies against TSG101 (ab125011, Abcam, Abcam, Cambridge, MA, USA), CD9 (ab307085, Abcam), CD63 (ab315108, Abcam), PTEN (ab32199, Abcam), Akt (ab8805, Abcam), p-Akt (ab38449, Abcam), p-mTOR (ab137133, Abcam), LC3B-I/II (ab192890, Abcam), PTEN induced kinase 1 (PINK1, ab216144, Abcam), Parkin (ab77924, Abcam), Cytochrome C (ab133504, Abcam), iNOS (BA0362, BOSTER, Wuhan, China), CD68 (BA3638, BOSTER), Arg1 (A01106, BOSTER), CD206 (A02285, BOSTER), DUSP1 (ab272587, Abcam), p-TAK1 (ab109404, Abcam), p-TAB2 (PA5-105086, Invitrogen), IKKβ (ab124957, Abcam), p-P65 (ab76302, Abcam), and β-actin (ab8226, Abcam), respectively. Finally, enhanced chemiluminescence (Beyotime) was used to visualize the target protein bands.

Enzyme-linked immunosorbent assay (ELISA)

The concentrations of inflammatory factors in supernatants and serum were detected by ELISA. IL-1α, IL-12, and TNF-α were detected using the corresponding ELISA kits (Solarbio, Beijing, China). Absorbance values (wavelength of 490 nm) were obtained with a spectrophotometer (Thermo Fisher Scientific). The concentrations of various inflammatory factors were calculated based on standard curves.

Transwell assays

After processing, the migration ability of HTR8-/Svneo cells was examined using Transwell chambers (Corning, Corning, NY, USA). Briefly, 5×10^4 cells resuspending in 100 μL serum-free medium were added to each upper Transwell chamber, and DMEM supplemented with 10% FBS (500 μL) was added to each lower chamber. After 24 h of culture, cells in the upper chambers were removed and the migrated cells were harvested. Next, the migrated cells were stained with 0.4% crystal violet and photographed under a light microscope (BX53, Olympus). For invasion assays, the Transwell chambers were pre-coated with Matrigel, but all other procedures were the same as those used for migration assays.

Flow cytometry (FCM)

HTR8-/Svneo cells (1×10^4) were treated with dihydroethidium to measure their levels of reactive oxygen species (ROS). In addition, an Annexin V-FITC/PI Apoptosis Detection Kit (Beyotime) was used to measure the levels of cell apoptosis. To detect the phenotype of macrophages, cells were incubated with antibodies targeting iNOS or Arg1. Isotype-matched antibodies were used to define background staining. Positive signals after staining were analyzed by flow cytometry (Thermo Fisher Scientific) and the data were treated with the software FlowJo (Version 10.9.0, TreeStar, Ashland, OR, USA).

Hoechst staining

To visualize cell apoptosis, cells were stained with Hoechst 33,342. Briefly, cells were added to 12-well plates that contained a coverslip in each well. After stimulation, the supernatants were removed, and the cells were fixed. Next, the cells were incubated with the staining solution (500 μL/well) for 10 min in the dark. Finally, positive signals were recorded under a fluorescence microscope (CKX53, Olympus).

Immunofluorescence

Cells were permeabilized with 0.5% Triton X-100, and subsequently fixed with 4% paraformaldehyde for 20 min. Following overnight blocking at 4ºC with 5% FBS, the cells were treated with a primary antibody, followed by treatment with a secondary antibody. Images of fluorescent cells were captured under a fluorescence microscope (CKX53, Olympus).

Dual-luciferase reporter assay

Dual-luciferase reporter assays were performed to detect a potential binding site for miR-141-3p on DUSP1. Psi-CHECK2 vectors containing the DUSP1 sequence (psi-CHECK2-DUSP1-WT) or mutant DUSP sequence (psi-CHECK2-DUSP1-MUT), an miR-141-3p mimic, or a short sequence without a target (as a negative control), were purchased from IGE Biotech (IGE Biotech, China). The miR-141-3p mimic or short sequence without a target was transiently transfected into HTR8-/Svneo cells using Lipofectamine 3000 (Beyotime). After 24 h, the dual fluorescent substrate (TransGen, Beijing, China) was added and luciferase activity was quantified under a fluorescence microscope (CKX53, Olympus).

Fluorescence in situ hybridization (FISH)

MR-141-3p engulfed by macrophages was detected by FISH. Briefly, cells were fixed 4% paraformaldehyde, and then hybridized in darkness with a miR-141-3p FISH probe, purchased from RIBO (Ribo Bio, China). Disordered sequence-probes were employed as negative controls. Finally, fluorescence images were captured under a fluorescence microscope (CKX53, Olympus).

Animal model

The protocols for all animal experiments were approved by the Animal Welfare Committee of Hainan Affiliated Hospital of Hainan Medical University (Med-Eth-Re [2022] 745), and the animals were processed in accordance with guidelines published by the National Institutes of Health, with guidance from the Animal and Institutional Animal Health and Use Committee. Female C57BL/6 mice (6 ~ 7 weeks old, $n = 24$) and male C57BL/6 mice (6 ~ 7 weeks old, $n = 8$) were provided by the Nanjing Biomedical Research Institute of Nanjing University and fed together in the same cage for 24 h. A female mouse was considered to be pregnant on day 1 if their vaginal plug was found the next morning. For grouping purposes, normal saline ($n = 8$), miR-141-3p agomir (10 nmol, $n = 8$), or miR-141-3p agomir (10 nmol) + antagomir (50 nmol, $n = 8$) was injected through the tail vein of the mice, respectively. The injections were repeated every 3 days until day 15. Eight female miR-141-3p-/-(KO) C57BL/6 mice and 16 female miR-141-3p+/+ C57BL/6 mice with the same background were provided by the Nanjing Biomedical Research Institute of Nanjing University and housed together with 8 male C57BL/6 mice for 24 h. The female mice were considered to be pregnant on day 1 if the vaginal plug was found the next morning. Pregnant miR-141-3p+/+ mice were randomly assigned to a control group ($n = 8$) or model group ($n = 8$). A PE model was constructed as described in a previous study[16]. Only female miR-141-3p-/-(KO) mice were used for the PE model. The blood pressure of each mouse was determined on days 5, 8, 11, 14, and 17 of pregnancy by the tail cuff method at the same time every morning. On day 18, each mouse was sacrificed by intraperitoneal injection of 0.5 mL of 1% pentobarbital sodium, and their placental tissue and serum were harvested.

Immunohistochemistry (IHC)

The placental tissues harvested from mice were embedded in paraffin and sectioned (4 μm). After dewaxing and rehydration, the endogenous peroxidase activity was blocked, and the tissues were treated with primary antibodies (anti-CD34 and anti-CD31 antibodies) and an HRP-conjugated secondary antibody. Finally, photographs were taken under a light microscope (BX53, Olympus).

Statistical analysis

All statistical analyses were performed using GraphPad Prism 8 (GraphPad Software, La Jolla, Ca, USA), and results are presented as the mean value ± standard error of the mean (SEM) of data obtained from at least three independent experiments. Comparative analyses between two groups were conducted using student's t-test, and comparisons among multiple groups were conducted using one-way analysis of variance and the Tukey's post hoc test. A P-value < 0.05 was regarded as being statistically significant.

Results

Hypoxia caused an abnormal elevation of miR-141-3p in HTR8-/Svneo cells

To explore the influence of hypoxia on miR-141-3p levels in trophoblasts, HTR8-/Svneo cells were stimulated with normoxia or hypoxia (Fig. 1A). Our results showed that the levels of miR-141-3p in the hypoxia group were significantly higher than those in the normoxia (control) group after 6 h of treatment (Fig. 1B). Moreover, cellular activity was inhibited by hypoxia (Fig. 1I). EVs were separated from the supernatants when cells had been treated for 24 h, and electron microscopy showed that their particle size was approximately 50 ~ 150 nm (Fig. 1C-D). TSG101, CD9, and CD63, expression in the supernatants was detected by western blotting (Fig. 1E), indicating the successful separation of EVs. The results also revealed that the levels of miR-141-3p in EVs were higher in the hypoxia group than in the control group (Fig. 1F). When the above-mentioned cells were cultured in new media under normoxic conditions for 24 h, the levels of miR-141-3p in both cells and EVs were still higher in the hypoxia group, demonstrating a continued effect of hypoxia on regulating miR-141-3p transcription in HTR8-/Svneo cells (Fig. 1G, H).

EVs derived from HTR8-/Svneo cells inhibited mitophagy

To investigate the influence of autocrine EVs on trophoblasts, HTR-8/Svneo cells were incubated with EVs isolated from the control and hypoxia groups under anoxic conditions. Results showed that the levels of miR-141-3p were significantly higher in the HTR-8/Svneo cells stimulated with EVs isolated from the control group (C-Exo) than with EVs isolated from the hypoxia group (H-Exo) (Fig. 2A). Interestingly, PTEN, a downstream factor of miR-141-3p, was downregulated, and phosphorylated AKT and phosphorylated mTOR were up-regulated in the H-Exo group (Fig. 2B). (Fig. 2C). Moreover, the levels of LC3B-II protein and mitochondrial autophagy-related proteins (PINK1 and Parkin) were also reduced in the H-Exo group (Fig. 2D). These findings suggest that EVs-derived miR-141-3p might restrain autophagy by targeting PTEN in trophoblasts. In addition, Cytochrome C expression and the levels of ROS and apoptosis were all increased in the H-Exo group when compared with the control group (Fig. 2E-G). Hoechst staining further revealed that cell apoptosis was stimulated in the H-Exo group (Fig. 2I). Furthermore, Transwell assays showed suppression of cell migration and invasion in the H-Exo group (Fig. 2H).

Cellular mitophagy induced by autocrine EVs was inhibited by miR-141-3p knockdown

To demonstrate the role of miR-141-3p in EVs-regulated mitophagy, EVs were separated from the supernatants under hypoxic conditions. Next, the cells were stimulated with EVs and transfected with an miR-141-3p

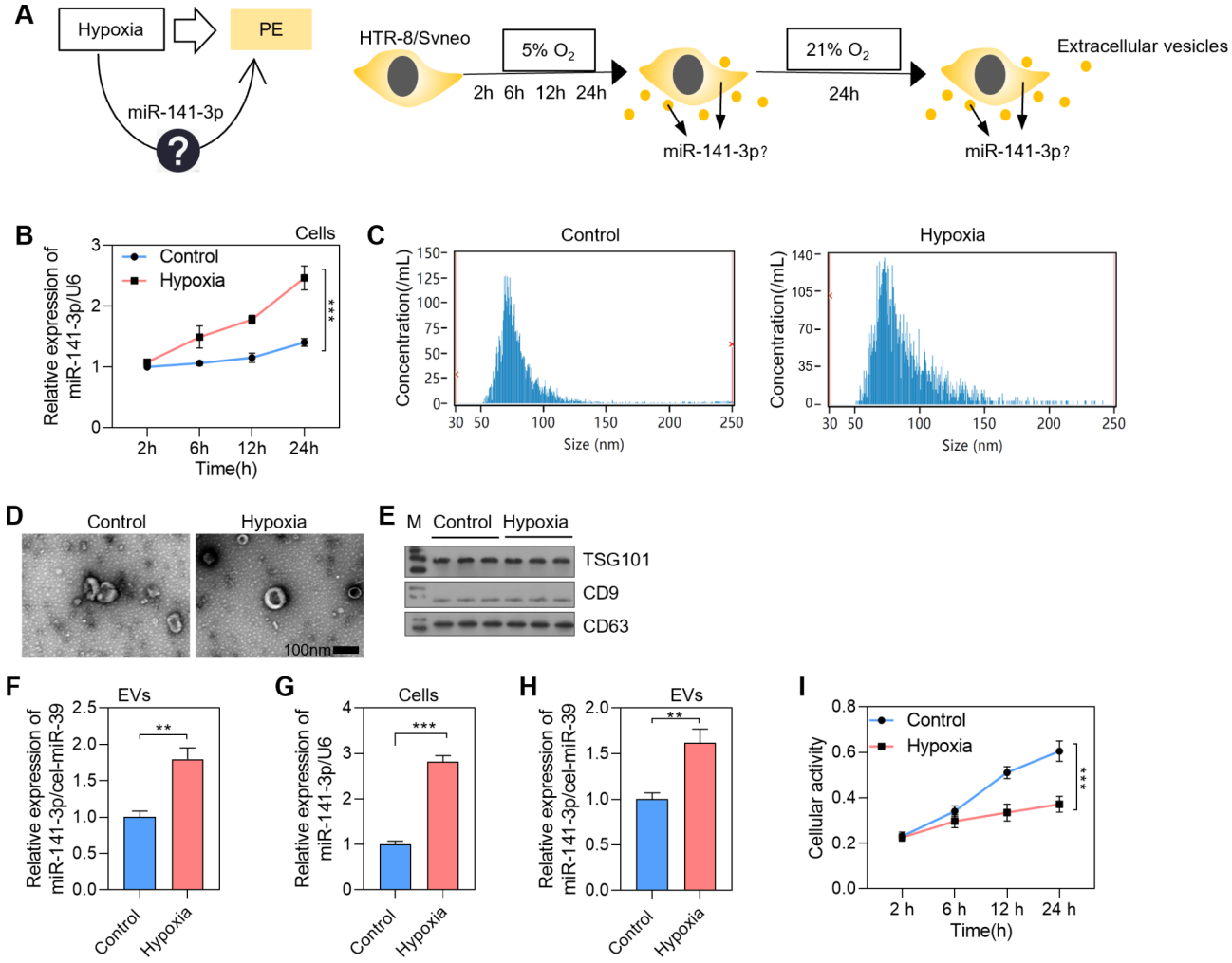

Fig. 1. The levels of miR-141-3p in trophoblast-derived EVs were up-regulated by hypoxia. **(A)** Schematic diagram showing the simulation of preeclampsia (PE) in vitro. **(B)** Relative expression of miR-141-3p in HTR-8/Svneo cells cultured under normoxic (Control) and hypoxic conditions for 2, 6, 12, and 24 h. **C**, **D.** The morphology of extracted EVs as detected by a NanoSight NS300 device and scanning electron microscope. **E.** Detection of EVs by western blotting analysis of exosome markers: TSG101, CD9, and CD63. **F.** HTR-8/Svneo cells were cultured under normoxic and hypoxic conditions for 24 h. Next, the culture medium was replaced and the cells were cultured for another 24 h under normoxic conditions. Finally, the EVs in the culture supernatant were extracted and relative levels of miR-141-3p expression were measured by qRT-PCR. **G**, **H.** HTR-8/Svneo cells were cultured under normoxic or hypoxic conditions for 24 h, and then cultured in new medium under normoxic conditions. The relative levels of miR-141-3p expression in cells and EVs were determined by qRT-PCR. **I.** The viability of HTR-8/Svneo cells cultured under normoxic conditions (Control) and hypoxic conditions for 2, 6, 12, and 24 h as detected by the CCK-8 assay. $^{**}p < 0.01$; $^{***}p < 0.001$.

inhibitor (H-Exo + inhibitor) or scramble (H-Exo + scramble). Results showed that the levels of miR-141-3p were markedly suppressed by its inhibitor (Fig. 3A). In addition, PTEN expression was increased, while p-Akt and p-mTOR expression were decreased in the H-Exo + inhibitor group (Fig. 3B). The numbers of autophagosomes were increased (Fig. 3C), and the levels of LC3B-II, PINK1, and Parkin were also increased in the H-Exo + inhibitor group (Fig. 3D). In addition, the levels of Cytochrome C expression, ROS, and cell apoptosis were all decreased in the H-Exo + inhibitor group when compared with the H-Exo + scramble group (Fig. 3E-G). Hoechst staining also revealed that cell apoptosis was decreased in the H-Exo + inhibitor group (Fig. 3I). Moreover, the degree of cell migration and invasion were both increased in the H-Exo + inhibitor group (Fig. 3H). Collectively, these results indicated that miR-141-3p in HTR8-/Svneo cell-derived EVs could inhibit mitophagy by targeting PTEN in HTR8-/Svneo cells (Fig. 3J).

Transfer of EVs from HTR8-/Svneo cells to THP-1-derived macrophages

When HTR-8/Svneo cells grown under normoxic or hypoxic conditions were co-cultured with THP-1-derived macrophages for 24 h (Fig. 4A), the expression of three inflammatory factors (IL-1α, IL-12, and TNF-α) was induced by hypoxia. Moreover, the secretion levels of those three factors by macrophages were far higher than

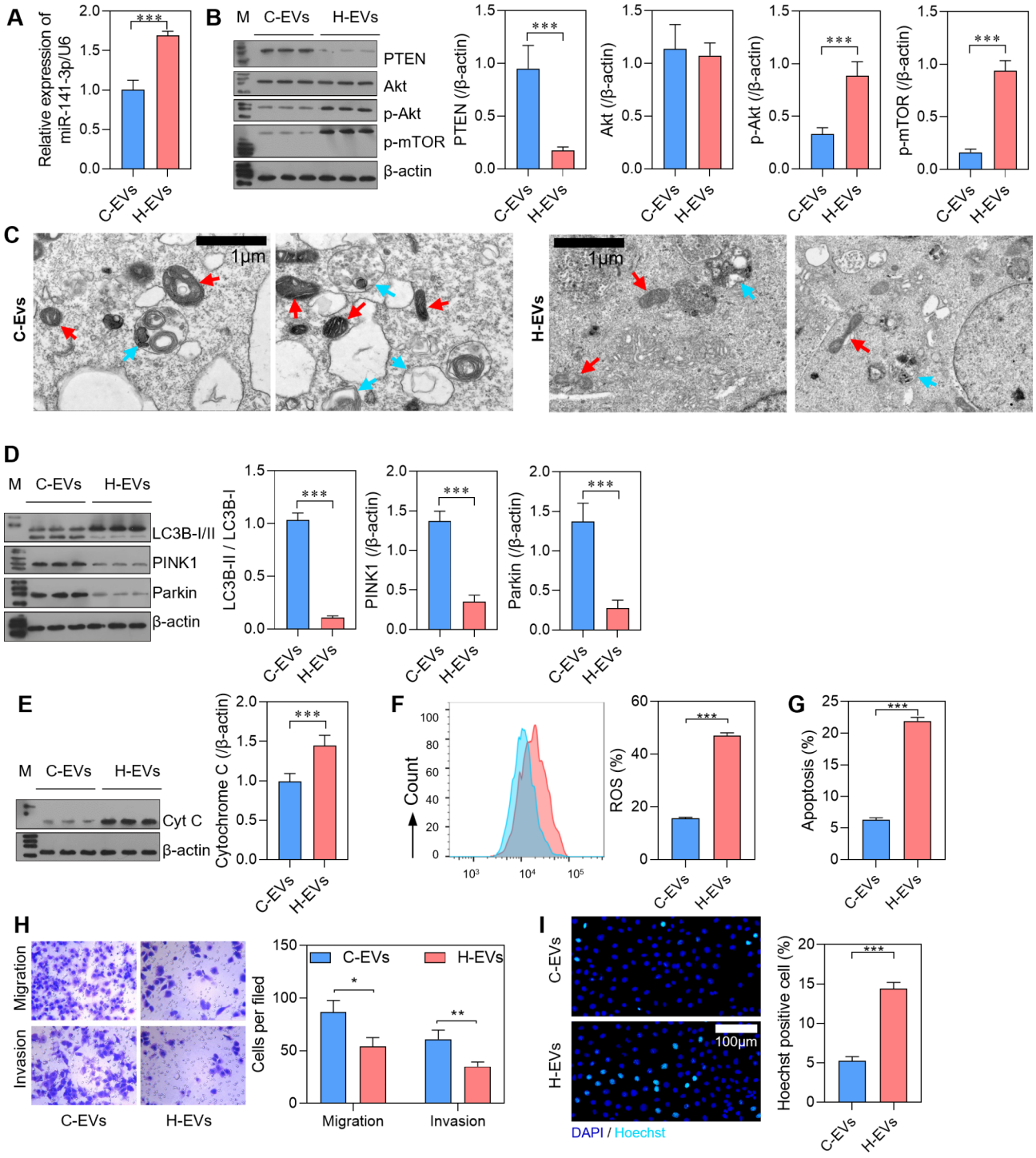

Fig. 2. Cellular mitophagy in HTR-8/Svneo cells was inhibited by autocrine EVs. HTR-8/Svneo cells were co-incubated with EVs from HTR-8/Svneo cells cultured under normoxic (C-Exo) or hypoxic (H-Exo) conditions for 24 h. **(A)** The relative levels of miR-141-3p expression in the C-Exo and H-Exo groups were detected by qRT-PCR. **(B)** Expression of the potential target of miR-141-3p, PTEN, and the expression of factors in the down-stream pathway. **(C)** The morphology of cells and autophagosomes as detected by transmission electron microscopy. The red arrow indicates mitochondria, while the yellow arrow indicates mitochondria engulfed by autophagosomes. **(D)** Detection of autophagy markers, LC3B-I/II, and 2 proteins involved in the mitochondrial autophagy pathway, PINK1 and Parkin, by western blotting. **(E)** Detection of cytoplasmic Cytochrome C by western blotting. **F**, **G.** Detection of ROS levels and apoptotic cells by flow cytometry. **H.** Cell migration and invasion abilities were detected by Transwell assays (magnification: 200×). **I.** Cell apoptosis as detected by Hoechst staining. $^{*}p < 0.05$; $^{**}p < 0.01$; $^{***}p < 0.001$.

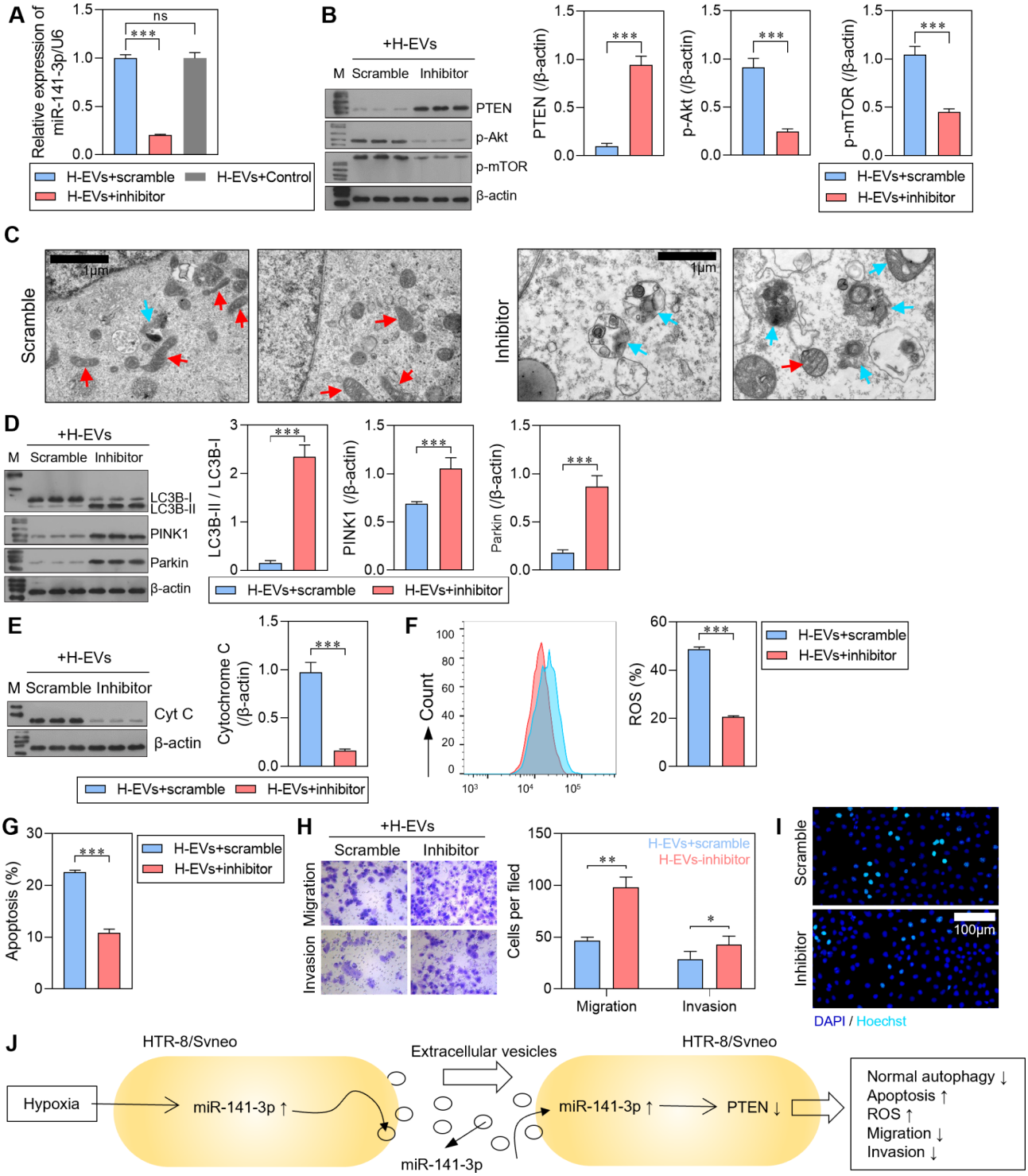

Fig. 3. Cellular mitophagy induced by autocrine EVs in HTR-8/Svneo cells was inhibited by an miR-141-3p inhibitor. HTR-8/Svneo cells were cultured with EVs from hypoxia-pre-treated HTR-8/Svneo cells and transfected with the miR-141-3p scramble (H-Exo + scramble) or inhibitor (H-Exo + inhibitor). **(A)** Relative expression of miR-141-3p in the H-Exo + scramble and H-Exo + inhibitor groups was detected by qRT-PCR. **(B)** The expression of PTEN and factors in the down-stream pathway. **(C)** The morphology of cells and autophagosomes was detected by transmission electron microscopy. The red arrow indicates mitochondria, while the yellow arrow indicates mitochondria engulfed by autophagosomes. **(D)** Detection of LC3B-I/II, PINK1, and Parkin by western blotting. **(E)** Detection of cytoplasmic Cytochrome C by western blotting. **F, G.** Detection of ROS levels and apoptotic cells by flow cytometry. **H.** Cell migration and invasion abilities were detected by Transwell assays (magnification: 200×). **I.** Cell apoptosis as detected by Hoechst staining. **J.** Schematic diagram showing the mechanism of miR-141-3p in HTR-8/Svneo cells. $^{*}p < 0.05$; $^{**}p < 0.01$; $^{***}p < 0.001$.

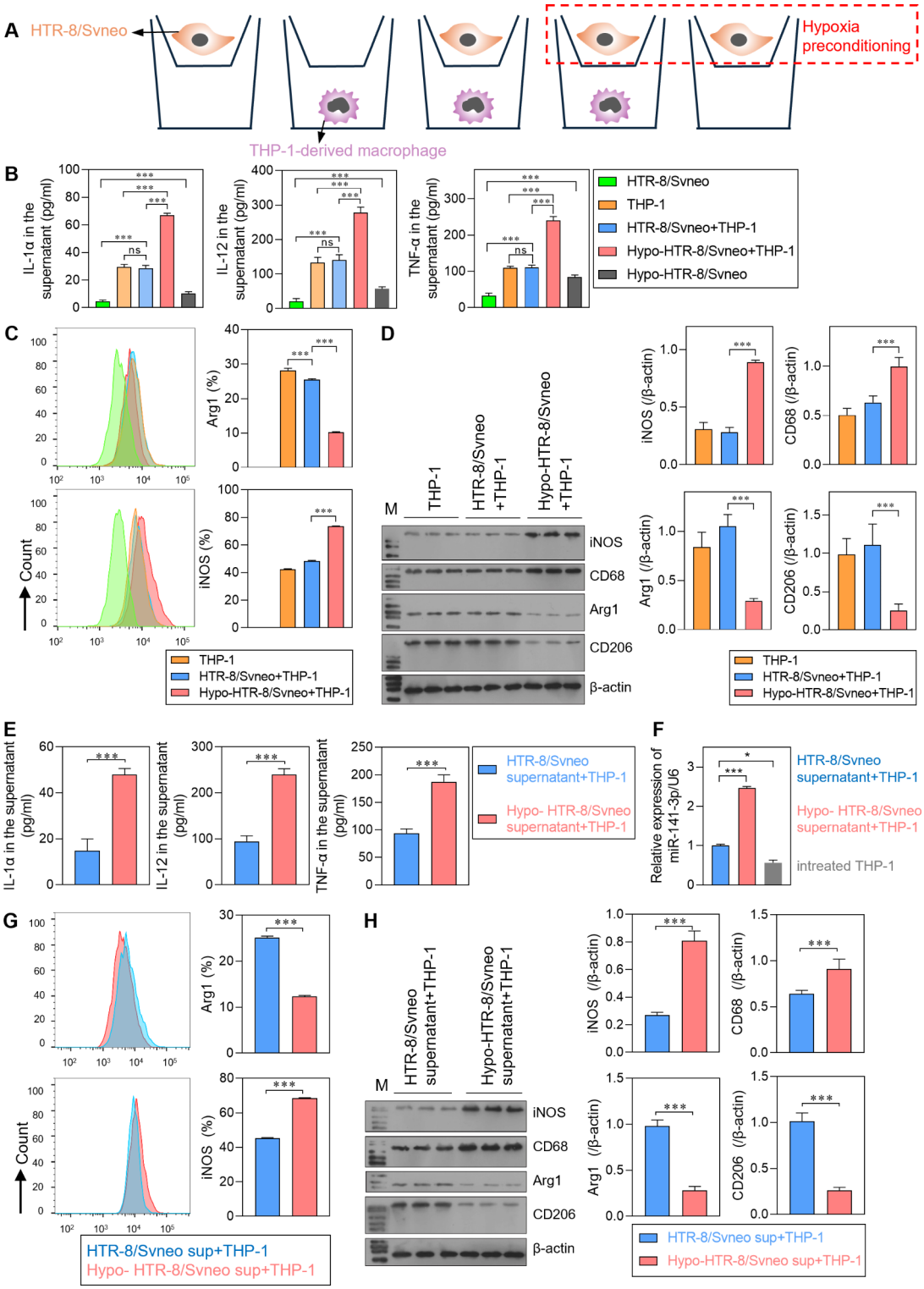

secretion from HTR-8/Svneo cells alone (Fig. 4B). This inferred that trophoblasts could stimulate the secretion of inflammatory-related factors by macrophages under hypoxic conditions. Flow cytometry revealed that the numbers of M1-macrophages (iNOS$^+$) were significantly elevated in the HTR-8/Svneo cells + THP-1 group, and were even further elevated in the Hypo-HTR-8/Svneo cells + THP-1 group. Meanwhile, the numbers of M2-macrophages (Arg1$^+$) showed an opposite trend (Fig. 4C). In addition, western blotting revealed that the expression of M1-macrophage markers (iNOS and CD68) was increased in the Hypo-HTR-8/Svneo cells + THP-1 group when compared with the HTR-8/Svneo cells + THP-1 group, while the expression levels of M2-macrophages markers (Arg1, CD206) showed the opposite trend (Fig. 4D). These findings indicated that HTR8-/Svneo cells could induce THP-1-derived macrophages to transform into the M1-phenotype, and hypoxia might be a factor that induces that transformation process.

◀**Fig. 4**. Effects of co-culture of trophoblasts and macrophages treated with hypoxia on cellular functions. **A.** THP-1-derived macrophages (lower chamber) were co-cultured with HTR-8/Svneo cells (upper chamber). **B.** The levels of IL-1α, IL-12, and TNF-α in cell supernatants were detected by ELISA. **C.** Identification of the macrophage phenotype by flow cytometry. **D.** Identification of the macrophage phenotype by western blot analysis of phenotype markers: iNOS and CD68 for the M1-phenotype; Arg1 and CD206 for the M2-phenotype. Furthermore, THP-1-derived macrophages were treated with the supernatants of hypoxia-pretreated or non-treated HTR-8/Svneo cells **E.** The levels of IL-1α, IL-12, and TNF-α in cell supernatants were detected by ELISA. **F.** Relative expression of miR-141-3p in macrophages. **G**. Identification of the phenotypes of macrophages by flow cytometry. **H.** Identification of the phenotypes of macrophages by western blot analysis: iNOS and CD68 for the M1-phenotype; Arg1 and CD206 for the M2-phenotype. HTR-8/Svneo: HTR-8/Svneo cells cultured alone; THP-1: THP-1-derived macrophages cultured alone; HTR-8/Svneo + THP-1: HTR-8/Svneo cells co-cultured with THP-1-derived macrophages; Hyo-HTR-8/Svneo + THP-1: hypoxia-treated HTR-8/Svneo cells co-cultured with THP-1-derived macrophages; HTR-8/Svneo supernatant + THP-1: THP-1-derived macrophages treated with supernatant from HTR-8/Svneo cells; Hypo-HTR-8/Svneo supernatant + THP-1: THP-1-derived macrophages treated with supernatant from hypoxia-treated HTR-8/Svneo cells. ns: no significance; $^{*}p < 0.05$, $^{***}p < 0.001$.

Macrophages were also cultured with the supernatants of HTR-8/Svneo cells grown under conditions of normoxia or hypoxia. Our data showed that supernatants from hypoxia-treated cells significantly promoted the secretion of IL-1α, IL-12, and TNF-α (Fig. 4E), and increased the proportions of M1-macrophages (Fig. 4G, H). Our results further revealed that the levels of miR-141-3p were higher in macrophages treated with the supernatants of HTR-8/Svneo cells grown under hypoxic conditions than under normoxic conditions (Fig. 4F). This suggested that miR-141-3p might be transferred from HTR8-/Svneo cells to THP-1-derived macrophages via EVs, and regulate the phenotype and function of macrophages.

HTR8-/Svneo cells regulated the polarization of THP-1-derived macrophages by secretion of miR-141-3p in EVs

To verify whether macrophages could absorb HTR8-/Svneo cell-derived EVs, EVs marked with PKH26 were incubated with THP-1-derived macrophages. When observed under a fluorescence microscope, fluorescence signals were detected in macrophages cultured with EVs from hypoxia-treated or normoxia-treated HTR-8/Svneo cells (Figure S1A). This demonstrated that macrophages could phagocytize EVs. Moreover, FISH assays revealed that the levels of miR-141-3p were higher in macrophages incubated with EVs from hypoxia-treated HTR-8/Svneo cells than in macrophages incubated with EVs from normoxia-treated HTR-8/Svneo cells. Furthermore, the miR-141-3p levels were also higher in macrophages incubated with EVs from the miR-141-3p mimics transfection group than in macrophages incubated with EVs from the hypoxia-treated group (Figure S1B). This suggested that the THP-1-derived macrophages had obtained the miR-141-3p from EVs.

We also knocked down miR-141-3p expression in trophoblasts cultured under hypoxic conditions, and then co-cultured them with macrophages. ELISA assays showed that the levels of IL-1α, IL-12, and TNF-α expression were decreased in the knockdown group (Inhibitor/ H-Exo) when compared with the scramble treated group (Scramble/H-Exo) (Fig. 5A). In addition, there were fewer M1-macrophages and higher numbers of M2-macrophages in the knockdown group (Fig. 5B, C). Coincidentally, our data also revealed that the levels of miR-141-3p were decreased in macrophages from the knockdown group (Fig. 5D).

A bioinformatic analysis showed that DUSP1 was a downstream target of miR-141-3p. The binding site is shown in Fig. 5E. A dual luciferase reporter assay had further proved that miR-141-3p could directly target DUSP1 (Fig. 5F). DUSP1 expression was decreased in macrophages co-cultured with the scramble and hypoxia treated group (Scramble/H-Exo) when compared to macrophages co-cultured with the scramble and normoxia treated group (Scramble/ C-Exo). Meanwhile, DUSP1 expression was increased in macrophages co-cultured with the miR-141-3p knockdown and hypoxia treated group (Inhibitor/H-Exo) when compared to macrophages co-cultured with the scramble and hypoxia treated group (Scramble/H-Exo) (Fig. 5G-I). In summary our data showed that DUSP1 expression was negatively correlated with miR-141-3p expression in macrophages.

Next, the miR-141-3p inhibitor or mimics were transfected into THP-1-derived macrophages to study the function of miR-141-3p in macrophages. When compared with the scramble treated group, the levels of IL-1α, IL-12, and TNF-α, the proportion of M1-macrophages, and the levels of miR-141-3p were all reduced in miR-141-3p inhibitor treated group, but were elevated in the miR-141-3p mimics treated group. Meanwhile, DUSP1 expression showed the opposite trends (Fig. 6A-D). We also detected the levels of DUSP1 protein and its down-stream factors. We found that the levels of DUSP1 protein were elevated in the miR-141-3p inhibitor treated group, and decreased in the miR-141-3p mimics treated group. The expression of down-stream factors, including phosphorylated (p-) TAK1, TAB2, IKKβ, and P65, showed the opposite trends (Fig. 6E). The correlation between DUSP1 expression and p-TAK1, p-TAB2 expression was also demonstrated by immunofluorescence (Figure S2). Taken together, our data suggest that miR-141-3p might regulate TAK1/TAB2 by targeting DUSP1, and ultimately affect THP-1-derived macrophage polarization by modulating the NF-κB/ p65 signaling pathway (Fig. 6F).

MiR-141-3p changed the phenotypes of macrophages in preeclampsia

We further investigated the role of miR-141-3p in vivo. The blood pressure of pregnant C57BL/6 mice with different treatments was measured by the tail-cuff method. Starting on day 11 of gestation, the blood pressure readings of mice treated with agomir were significantly higher than those of mice injected with agomir + antagomir or mice from the control group (Fig. 7A). We also found that the levels of miR-141-3p were increased in the

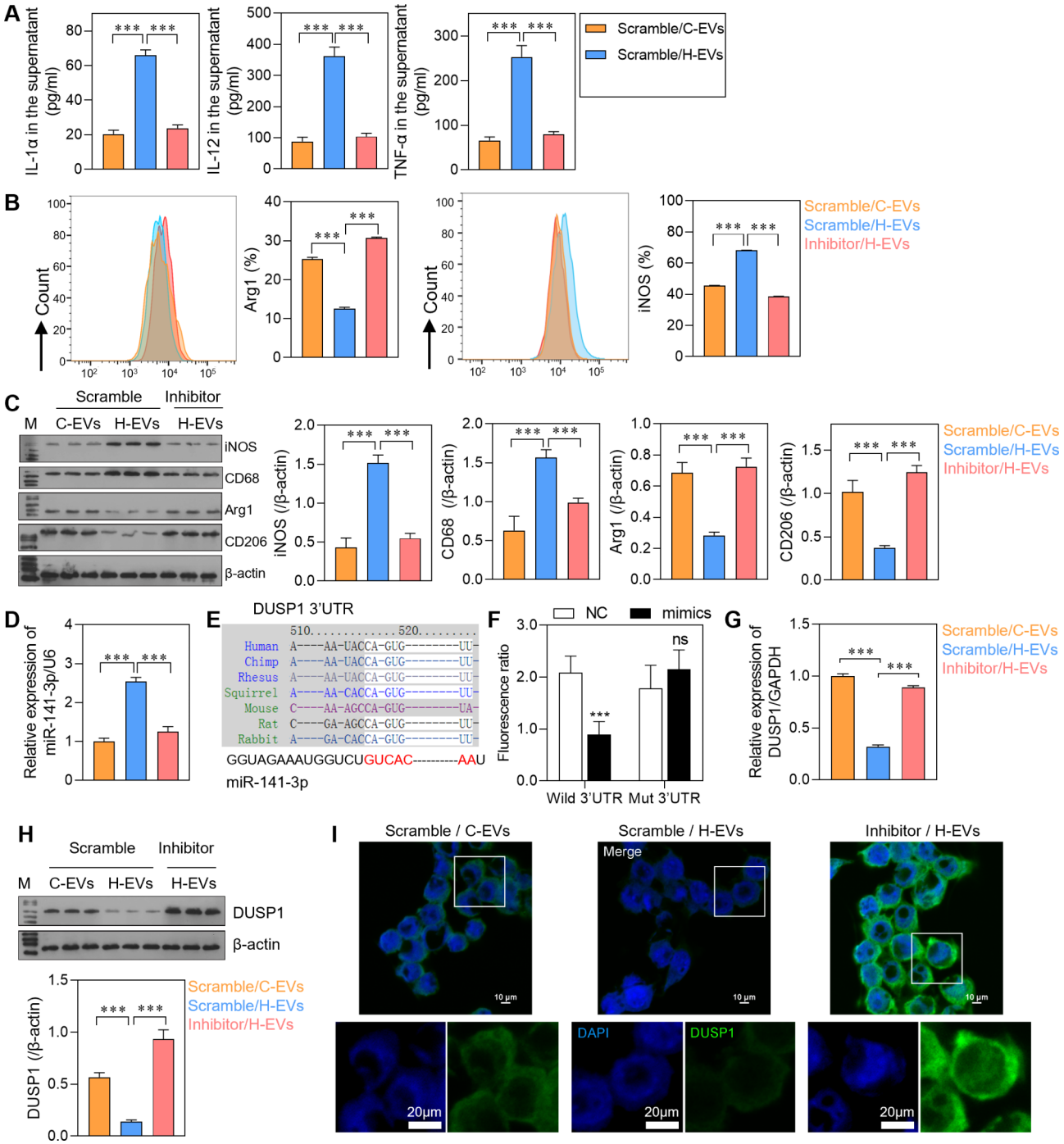

Fig. 5. MiR-141-3p in HTR-8/Svneo-derived EVs regulated the phenotype of macrophages. THP-1-derived macrophages were stimulated with hypoxia-treated HTR-8/Svneo-derived EVs for 24 h. **A.** The levels of IL-1α, IL-12, and TNF-α in supernatants were detected by ELISA. **B**, **C.** Identification of the phenotypes of macrophages by flow cytometry and western blotting. **D.** Relative expression of miR-141-3p in macrophages. **E.** The predicted binding site of miR-141-3p on the DUSP1 3'UTR sequence. **F.** A dual-luciferase reporter assay was performed to examine the binding site. **G-I.** DUSP1 expression was detected by qRT-PCR, western blotting, and immunofluorescence. Scramble/ C-Exo: THP-1 derived macrophages transfected with scramble were cultured with EVs from HTR-8/Svneo cells. Scramble/ H-Exo: THP-1 derived macrophages transfected scramble were cultured with EVs from hypoxia-treated HTR-8/Svneo cells. Inhibitor/H-Exo: THP-1 derived macrophages transfected with the miR-141-3p inhibitor were cultured with the supernatants from hypoxia-treated HTR-8/Svneo cells. ns: no significance; $^{***}p < 0.001$.

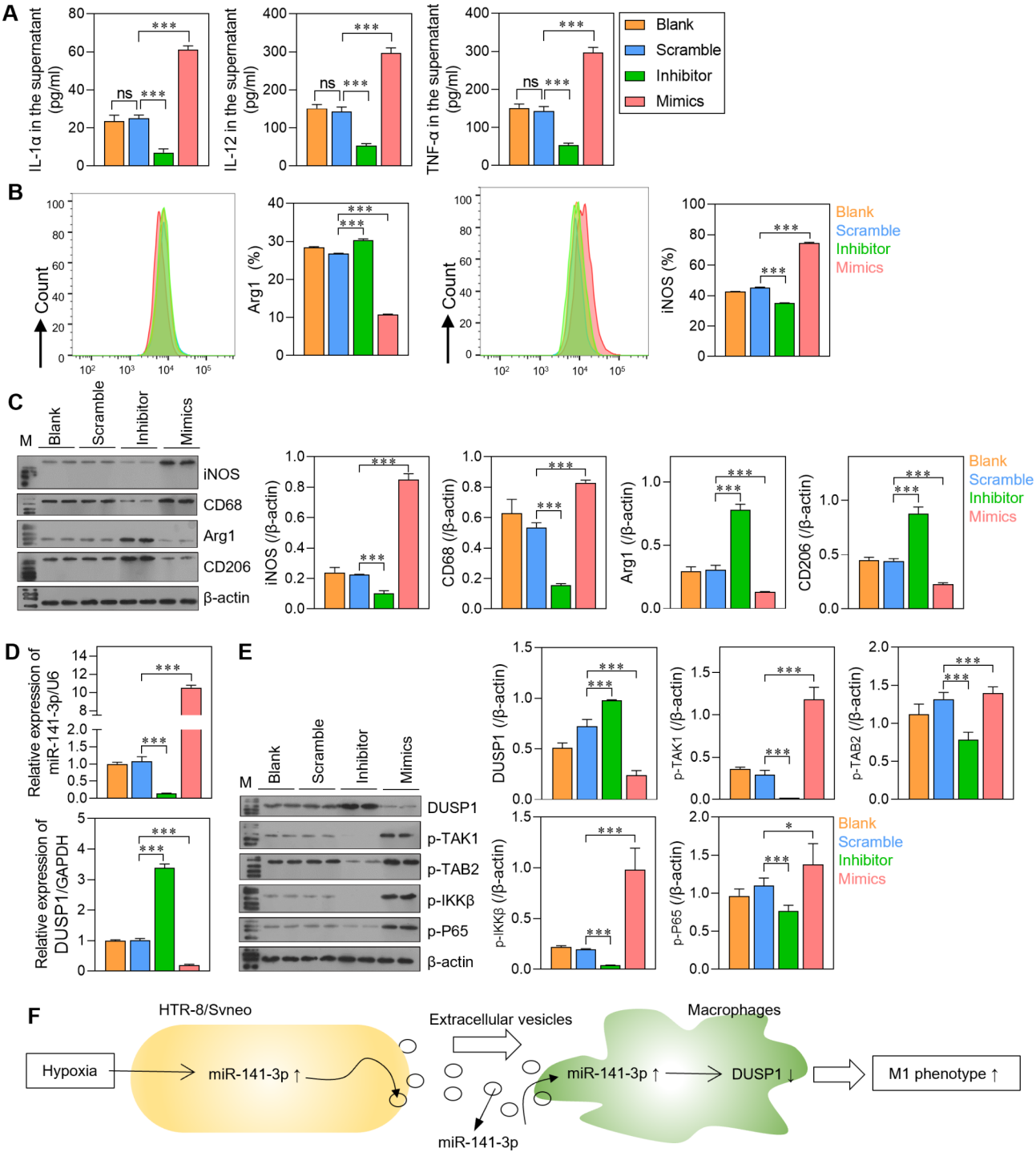

Fig. 6. The effect of miR-141-3p on macrophages. Macrophages were directly transfected with the miR-141-3p inhibitor or mimics for 24 h. **A.** The levels of IL-1α, IL-12, and TNF-α in supernatants were detected by ELISA. **B**, **C.** Identification of the macrophage phenotype by flow cytometry and western blotting. **D.** Relative expression of miR-141-3p and DUSP1 in macrophages. **E.** The expression of DUSP1 and phosphorylated proteins in the down-stream pathway as detected by western blotting. **F.** Schematic diagram showing the mechanism of miR-141-3p obtained from HTR-8/Svneo-derived EVs in macrophages. ns: no significance; $^{*}p < 0.05$; $^{***}p < 0.001$.

trophoblasts and decidua of mice treated with agomir, but decreased in the trophoblasts and decidua of mice injected with agomir + antagomir when compared to levels of miR-141-30 in the trophoblasts and decidua of mice injected with agomir alone (Fig. 7C). Moreover, the levels of IL-1α, IL-12, TNF-α, iNOS, CD86, p-TAK1, p-TAB2, p-IKKβ, and p-P65 displayed the same trend as that of miR-141-3p, while the levels of Arg1, CD206,

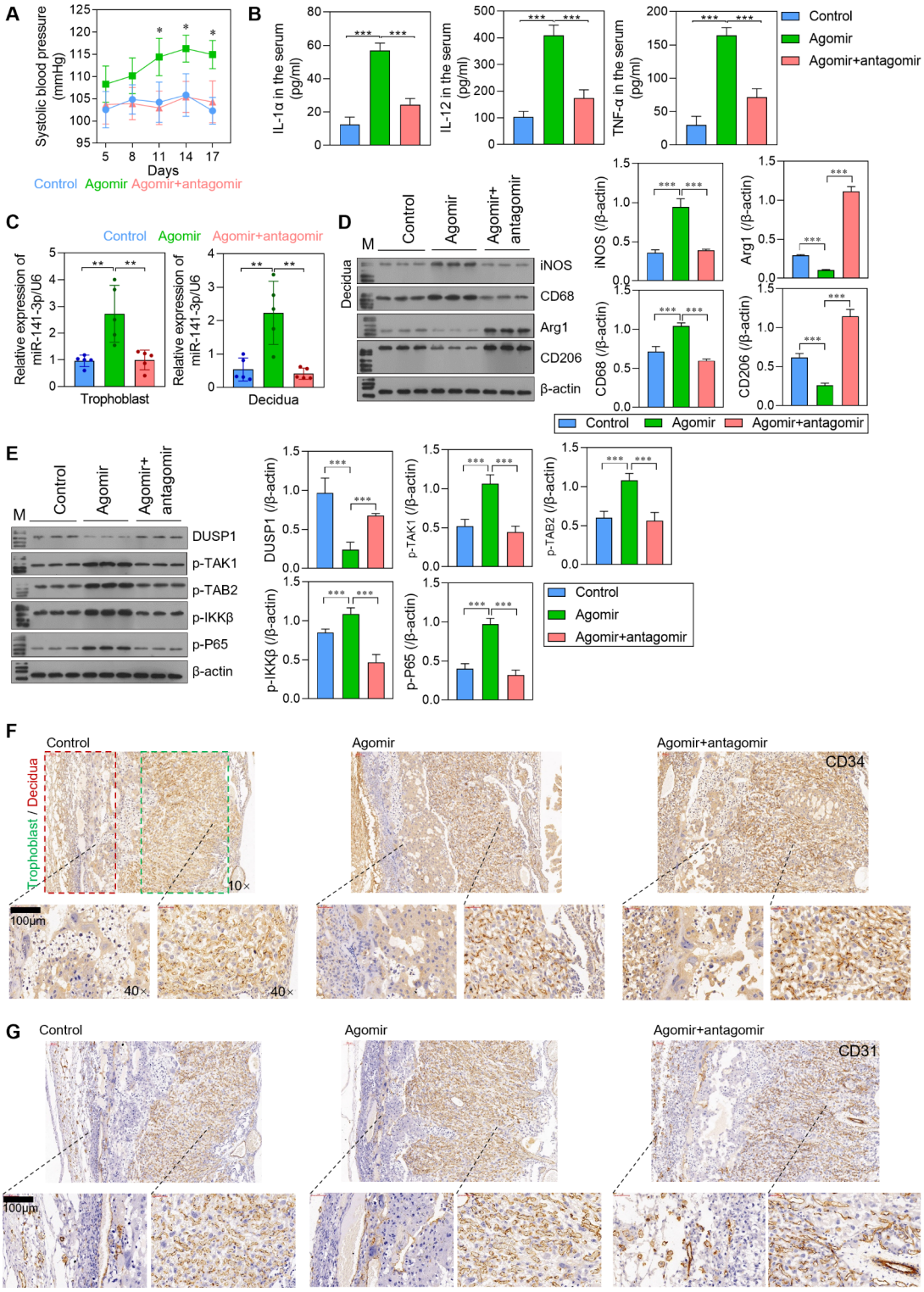

Fig. 7. The effect of miR-141-3p on regulation of the macrophage phenotype in pregnant mice. **(A)** Blood pressure was detected on days 5, 8, 11, 14, and 17 of pregnancy using a tail cuff. **(B)** The levels of IL-1α, IL-12, and TNF-α in serum were detected by ELISA. **(C)** Relative levels of miR-141-3p expression in trophoblasts and decidua tissues. **(D)** The phenotypes of macrophages in decidua tissues were detected by western blotting. **(E)** The expression of DUSP1 and phosphorylated proteins in the down-stream pathway. **(F)** The placental vasculogenesis markers, CD31 and CD34, as detected by immunohistochemistry. $^{*}p < 0.05$; $^{**}p < 0.01$; $^{***}p < 0.001$.

and DUSP1 showed the opposite trend (Fig. 7B, D, E). The positive rates of angiogenesis biomarkers (CD31and CD34) were decreased in the decidua of mice injected with agomir, but those decreases were relieved in the decidua of mice injected with agomir + antagomir (Fig. 7F, G).

We also constructed a PE model with miR-141-3p-/- and miR-141-3p+/+ mice. Starting on day 8 of gestation, the blood pressure readings of the miR-141-3p-/- PE mice were higher than those of the healthy miR-141-3p+/+ mice (control), and the miR-141-3p+/+ PE mice had the highest blood pressure readings (Fig. 8A). In addition, the levels of IL-1α, IL-12, TNF-α, iNOS, CD86, p-TAK1, p-TAB2, p-IKKβ, and p-P65 were significantly elevated in the miR-141-3p+/+ PE mice, while the levels of Arg1, CD206, and DUSP1 expression were downregulated. Of note, the above effects were attenuated in the miR-141-3p-/- PE mice (Fig. 8B-D). Our IHC results showed that the positive rates of angiogenesis biomarkers (CD31and CD34) were reduced in the decidua from miR-141-3p+/+ PE mice, and those reductions were relieved in the decidua from miR-141-3p-/- PE mice (Fig. 8E, F).

Discussion

The mechanism of PE is complex. Understanding the pathogenesis of PE will help to prevent and treat the disease. Currently, researchers are paying greater attention to intercellular communications that occur between trophoblast cells and immune cells in the placenta[17]. They found that an abnormal interaction between macrophages and trophoblasts may lead to spiral artery reshaping failure and defective placental development in women with PE[18]. Therefore, it is of great importance to demonstrate the relationship between macrophages and trophoblast cells in decidual tissue in order to understand the pathological mechanism and proper treatment for PE. Here, we found that miR-141-3p from HTR8-/Svneo cell-derived EVs could inhibit the transfer capability of those cells and regulate the polarization of THP-1-derived macrophages in vitro (Fig. 9).

Macrophages are the main immune cells involved in the entire process of pregnancy. They play a vital role in placental maintenance, and reshaping of the spiral arteries[18]. Their normal function is an important factor in maintaining the proper microenvironment; otherwise, an excessive inflammatory response adverse to trophoblast growth and survival could cause irreversible damage to the fetus[19]. Dysfunction of DMs is associated with the occurrence of PE. Abnormalities in macrophages affect their interaction with other constituent cells in the placenta, which subsequently disorders the original immune system and leads to PE[20]. In addition, abnormal gene expression in macrophages can reduce the adhesion between macrophages and trophoblast cells, and shrink the junction area and placenta during pregnancy[21]. Mor et al.[22] found that the communication that occurs between trophoblast cells and macrophages is vital for protecting the fetus. The migration and infiltration of macrophages are increased by trophoblast cells. Consistent with those findings, when we extracted HTR-8/Svneo cell-derived EVs and incubated them with THP-1-derived macrophages, our results showed that both hypoxia-treated HTR-8/Svneo cells and EVs could increase the secretion of proinflammatory factors from macrophages by regulating M1/M2 polarization. Macrophages maintain an active but tolerant immune microenvironment that is essential for maternal immune tolerance to the fetus, and for vasculature remodeling, trophoblast growth, and survival. Liu et al.[23]. found that macrophages in the preeclamptic placenta were mainly of the M1 phenotype, which resulted in an inflammatory environment in the placenta. Moreover, extracellular vesicles derived from trophoblasts of PE patients were found to up-regulate the proportion of M1-macrophages when compared with macrophages from women with normal pregnancies. In the current study, THP-1-derived macrophages were found to induce M1 polarization by HTR-8/Svneo cell-derived EVs in vitro, which may be related to a hypoxia-promoted upregulation of miR-141-3p in EVs. This suggests that trophoblast cells may cause an imbalance of macrophage polarization by secreting certain substances contained in extracellular vesicles. Therefore, the phenotypes of macrophages might regulate the invasion of trophoblast cells. In turn, trophoblast cells might modulate the polarization of macrophages.

Extracellular vesicles seem to have a vital role in intercellular communications. They are classified based on their size. The EVs are extracellular vesicles with a size of 30–150 nm[24]. EVs contain lipids, proteins, and RNA molecules. They are derived from the exocytosis of multivesicular bodies, or are formed during the budding of cell membranes. Once they are released, EVs fuse with target cells to deliver biological signals that regulate the physiological processes of target cells[25] via autocrine and paracrine mechanisms. The substances transmitted by EVs may have a significant impact on the early placental development environment[26]. A previous study reported that preeclampsia-derived EVs could imbalance the activity of Th17 and Treg in peripheral blood mononuclear cells from healthy pregnant women[27]. Our results suggest that miR-141-3p derived from EVs may induce an inflammatory environment in the early placenta. EVs from PE patients were found to induce endothelial dysfunction and PE-like adverse symptoms in pregnant mice by delivering single Fms, such as Tyrosine Kinase-1 and single endoglin[28]. Mesenchymal stem cell-derived EVs can also transfer the long noncoding RNA MALAT1-201 to regulate trophoblast cell proliferation, apoptosis, and migration by targeting miR-141[29]. EVs from trophoblast cells can mediate macrophage recruitment and polarization in a cell-contact-independent manner[30]. In addition, due to the stable information carrying capability and excellent cargo transport capacity of EVs, they might serve as novel diagnostic markers for PE. It can be seen that EVs participate in interactions between not only trophoblasts and macrophages, but also between other types of cells in the placenta. However, to gain an understanding of the mechanism of intercellular information exchange that occurs during the development of preeclampsia, further studies must be conducted.

A previous study revealed that miR-141-3p levels were elevated in the placentas and plasma of PE patients[31], which suppressed trophoblast cell proliferation and invasion. In this study, we found that hypoxia altered miR-141-3p expression in HTR-8/Svneo cells, as well as its emission in the form of EVs. Another study found that methylation of the miR-141-3p promoter influenced miR-141-3p expression[32]. A reduction of miR-141-3p promoted cell metastasis and reduced the apoptosis of human umbilical vein endothelial cells cultured under hypoxic conditions[33]. MiR-141-3p was also found to be related to the invasion of cancer cells, such as thyroid cancer cells[34] and osteosarcoma cells[35]. Our results suggest that autocrine miR-141-3p inhibits HTR-8/Svneo

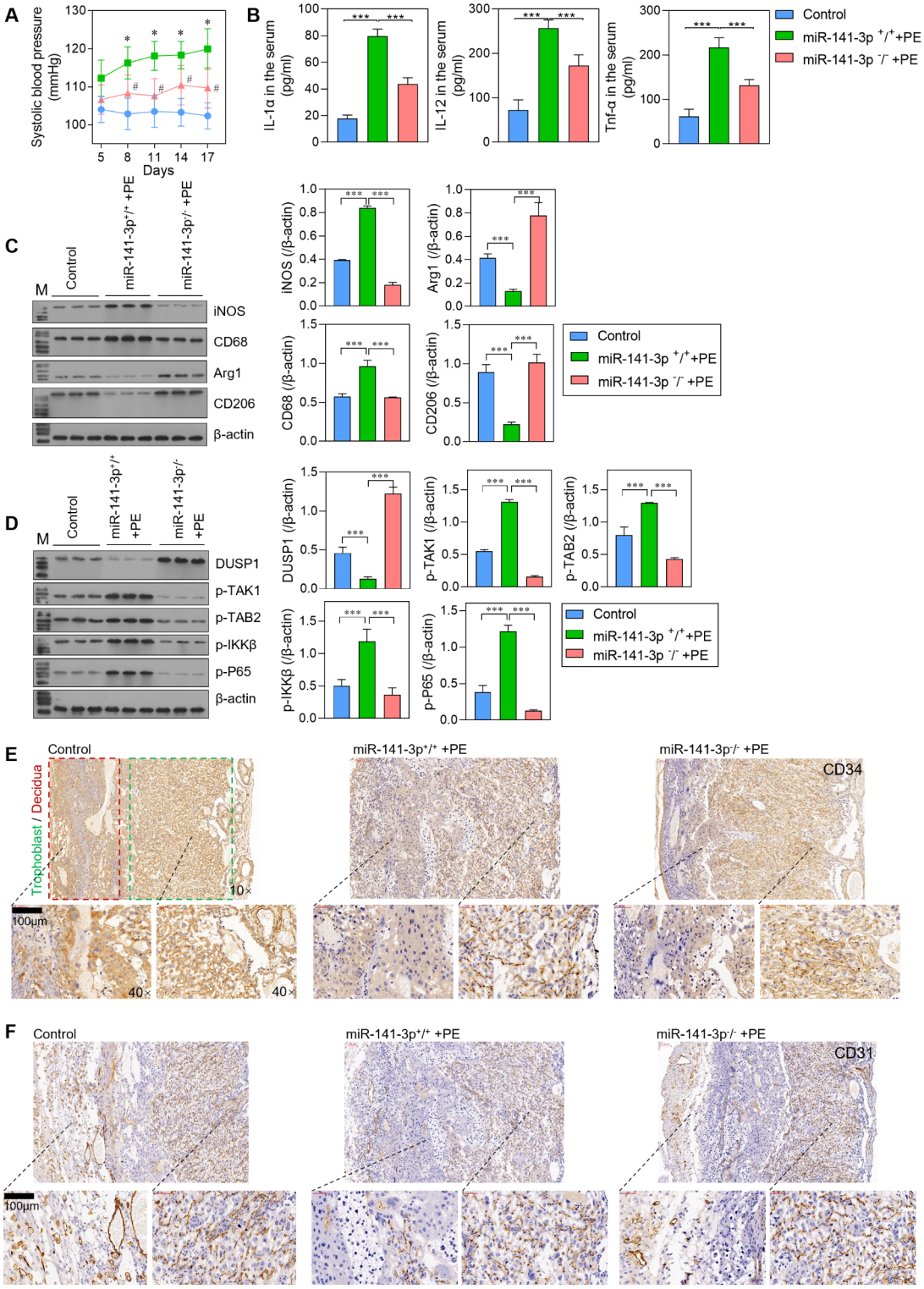

Fig. 8. The effect of miR-141-3p on regulation of the macrophage phenotype in preeclampsia mice. MiR-141-3p-/-(KO) C57BL/6 mice were used for induction of a PE model. **(A)** Blood pressure was detected on days 5, 8, 11, 14, and 17 of pregnancy using a tail cuff. **(B)** The levels of IL-1α, IL-12, and TNF-α in serum were detected by ELISA. **(C)** The phenotypes of macrophages in decidua tissues were detected by western blotting. **(D)** The expression of DUSP1 and phosphorylated proteins in the down-stream pathway. **(E)** The placental vasculogenesis markers, CD31 and CD34, as detected by immunohistochemistry. ***$p < 0.001$.

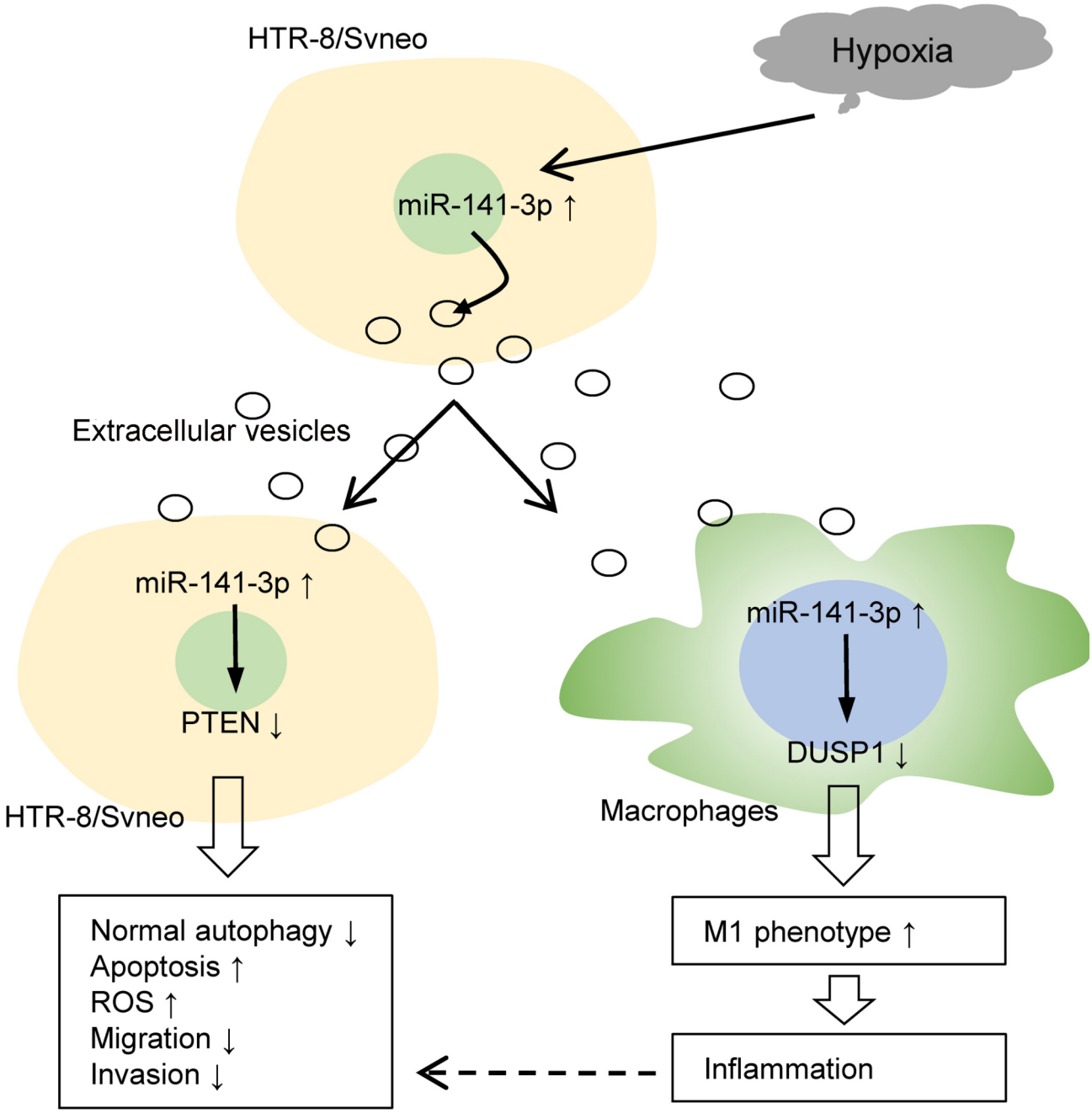

Fig. 9. Schematic diagram of the role of miR-141-3p derived from extracellular vesicles in preeclampsia in hypoxic environment.

cell metastasis and mitophagy in trophoblasts via a PTEN-AKT-mTOR axis. In addition, we revealed for the first time that paracrine miR-141-3p induces macrophage polarization to the M1-phenotype, which means that miR-141-3p may have a role in macrophage polarization and angiogenesis in decidual tissues from normal and PE mice.

DUSP1 is a dual threonine/tyrosine phosphatase. Herein, we found that DUSP1 is a downstream factor of miR-141-3p secreted by HTR-8/Svneo cells. In macrophages, downregulation of DUSP1 increases the number of proinflammatory M1-macrophages[36]. Köröskényi et al.[37] found that the adenylate A2A receptor signal could regulate macrophage polarization and function via DUSP1. Collectively, DUSP1 plays an important role in the polarization of macrophages. Yang et al.[38] found that DUSP1 expression was remarkably reduced in PE pregnant women when compared with healthy pregnant women. Similarly, our results suggest that DUSP1 expression is associated with the M1/M2 polarization of macrophages, and that association could be regulated by cellular interactions. Therefore, trophoblasts might regulate macrophage polarization via miR-141-3p targeting DUSP1.

Hypoxia caused by a failure of spiral artery remodeling is a common characteristic of PE. Oxidative stress can lead to ROS production in cells and induce mitochondrial dysfunction[39]. Mitophagy, a significant mitochondrial quality control mechanism, can prevent excessive ROS production by eliminating impaired mitochondria[40]. However, PE mice have a reduced level of mitophagy, as well as mitochondrial dysfunction in their placentas[41,42]. We found that EVs from hypoxia-treated HTR-8/Svneo cells could inhibit autophagy occurrence in trophoblasts. Meanwhile, PINK1 and Parkin ROS levels, as well as cytochrome C levels and apoptosis were all increased by EVs derived from hypoxia-treated HTR-8/Svneo cells. The PINK1-Parkin pathway is induced by PTEN and plays an important role in regulating mitophagy to compensate for acute mitochondrial dysfunction[43]. This pathway can be inhibited by EVs from hypoxia-treated HTR-8/Svneo; however, miR-141-3p knockdown can offset that suppressive effect. In addition, PTEN was found to be a target of miR-141-3p. This infers that trophoblast cells can reduce their levels of mitophagy via autocrine miR-141-3p targeting PTEN. Here, we demonstrated a novel mechanism involving interaction between trophoblast cells and macrophages. This mechanism may be helpful for understanding the pathogenesis of PE and developing proper therapies for the disease. However, a key limitation of this study lies in the potential for the developmental disparities between the human and mouse placenta to undermine the persuasiveness of the results. Separating primary trophoblast cells from early human placenta or monocytes from whole blood and conducting experiments in larger mammals with closer human affinity may be more beneficial for exploring the pathological mechanisms of PE.

Conclusion

Our in vitro data and PE mouse model data showed that trophoblast cell-derived miR-141-3p could inhibit cell migration, invasion, and mitophagy, and promote apoptosis by targeting PTEN. In macrophages, miR-141-3p was found to promote the transformation of macrophages into the M1-phenotype by targeting DUSP1. Cellular interaction between trophoblast cells and macrophages may play an important role in the pathological development of PE.

Data availability

All data generated or analysed during this study are included in this published article [and its supplementary information files].

Received: 19 December 2023; Accepted: 15 October 2024
Published online: 18 October 2024

References

1. Chappell, L. C., Cluver, C. A., Kingdom, J. & Tong, S. Pre-eclampsia. *Lancet*. **398** (10297), 341–354 (2021).
2. Ogoyama, M. et al. Non-coding RNAs and prediction of Preeclampsia in the first trimester of pregnancy. *Cells*. **11**, 15 (2022).
3. Lala, P. K. & Nandi, P. Mechanisms of trophoblast migration, endometrial angiogenesis in preeclampsia: the role of decorin. *Cell. Adh Migr.* **10**(1–2), 111–125 (2016).
4. Chen, D. B. & Wang, W. Human placental microRNAs and preeclampsia. *Biol. Reprod.* **88**(5), 130 (2013).
5. Pineles, B. L. et al. Distinct subsets of microRNAs are expressed differentially in the human placentas of patients with preeclampsia. *Am. J. Obstet. Gynecol.* **196**(3), 261e261–261e266 (2007).
6. Zhu, X. M., Han, T., Sargent, I. L., Yin, G. W. & Yao, Y. Q. Differential expression profile of microRNAs in human placentas from preeclamptic pregnancies vs normal pregnancies. *Am. J. Obstet. Gynecol.* **200**(6), 661e661–661e667 (2009).
7. Nishi, K. & Modi, D. Placental exosomes in pregnancy and preeclampsia. *Am. J. Reprod. Immunol.* **91**(5), e13857 (2024).
8. Yang, L. P., Zheng, J. H., Zhang, J. K. & Huang, X. Dysregulated miR-222-3p in plasma exosomes of preeclampsia patients and its In vitro effect on HTR8/SVneo extravillous trophoblast cells by targeting STMN1. Human and Experimental Toxicology. ; 2022 (41): 1–5. (2022).
9. Chen, Z. et al. Plasma exosomal miR-199a-5p derived from preeclampsia with severe features impairs endothelial cell function via Targeting SIRT1. *Reproductive Sci.* **29**(12), 3413–3424 (2022).
10. Vishnyakova, P. et al. MicroRNA miR-27a as a possible regulator of anti-inflammatory macrophage phenotype in preeclamptic placenta. *Placenta*. **145**, 151–161 (2024).
11. Zhou, H. et al. Downregulation of miR-92a in decidual stromal cells suppresses Migration ability of trophoblasts by promoting macrophage polarization. *DNA Cell. Biology*. **42**(8), 507–514 (2023).
12. Ospina-Prieto, S. et al. MicroRNA-141 is upregulated in preeclamptic placentae and regulates trophoblast invasion and intercellular communication. *Transl Res*. **172**, 61–72 (2016).
13. Liu, X. et al. Decidual macrophage M1 polarization contributes to adverse pregnancy induced by Toxoplasma Gondii PRU strain infection. *Microb. Pathog.* **124**, 183–190 (2018).
14. Buckley, R. J., Whitley, G. S., Dumitriu, I. E. & Cartwright, J. E. Macrophage polarisation affects their regulation of trophoblast behaviour. *Placenta*. **47**, 73–80 (2016).
15. Wu, D. et al. Hypoxia-induced microRNA-141 regulates trophoblast apoptosis, invasion, and vascularization by blocking CXCL12β/CXCR2/4 signal transduction. *Biomed. Pharmacother.* **116**, 108836 (2019).
16. Kanayama, N., Tsujimura, R., She, L., Maehara, K. & Terao, T. Cold-induced stress stimulates the sympathetic nervous system, causing hypertension and proteinuria in rats. *J. Hypertens.* **15**(4), 383–389 (1997).
17. Deer, E. et al. The role of immune cells and mediators in preeclampsia. *Nat. Rev. Nephrol.* **19**(4), 257–270 (2023).
18. Lu, H. Q. & Hu, R. The role of immunity in the pathogenesis and development of pre-eclampsia. *Scand. J. Immunol.* **90**(5), e12756 (2019).
19. Vishnyakova, P. et al. Preeclampsia: inflammatory signature of decidual cells in early manifestation of disease. *Placenta*. **104**, 277–283 (2021).
20. Rong, M., Yan, X., Zhang, H., Zhou, C. & Zhang, C. Dysfunction of decidual macrophages is a potential risk factor in the occurrence of Preeclampsia. *Front. Immunol.* **12**, 655655 (2021).
21. Przybyl, L. et al. CD74-Downregulation of placental macrophage-trophoblastic interactions in Preeclampsia. *Circ. Res.* **119**(1), 55–68 (2016).
22. Zhang, Y. H. et al. Trophoblast-secreted soluble-PD-L1 modulates macrophage polarization and function. *J. Leukoc. Biol.* **108**(3), 983–998 (2020).
23. Liu, X. et al. Trophoblast-derived extracellular vesicles promote Preeclampsia by regulating macrophage polarization. *Hypertension* **79**(10), 2274–2287 (2022).

24. Théry, C. et al. Molecular characterization of dendritic cell-derived exosomes. Selective accumulation of the heat shock protein hsc73. *J. Cell. Biol.* **147**(3), 599–610 (1999).
25. Mathivanan, S., Ji, H. & Simpson, R. J. Exosomes: extracellular organelles important in intercellular communication. *J. Proteom.* **73**(10), 1907–1920 (2010).
26. Chen, C. et al. Exosomes: New regulators of reproductive development. Materials Today Bio. ; 19: 100608. (2023).
27. Pourakbari, R. et al. Preeclampsia-Derived Exosomes Imbalance the activity of Th17 and Treg in PBMCs from healthy pregnant women. *Reproductive Sci.* **30**(4), 1186–1197 (2023).
28. Chang, X. et al. Exosomes from Women with Preeclampsia Induced Vascular Dysfunction by delivering sFlt (Soluble Fms-Like Tyrosine Kinase)-1 and sEng (Soluble Endoglin) to endothelial cells. *Hypertension*. **72**(6), 1381–1390 (2018).
29. Chen, F., Chen, X., Cai, W., Ruan, H. & Fang, S. Mesenchymal stem cell-derived Exosomal Long Noncoding RNA MALAT1-201 regulated the proliferation, apoptosis and Migration of Trophoblast cells via Targeting miR-141. *Ann. Clin. Lab. Sci.* **52**(5), 741–752 (2022).
30. Atay, S., Gercel-Taylor, C., Suttles, J., Mor, G. & Taylor, D. D. Trophoblast-derived exosomes mediate monocyte recruitment and differentiation. *Am. J. Reprod. Immunol.* **65**(1), 65–77 (2011).
31. Cao, G., Cui, R., Liu, C. & Zhang, Z. MicroRNA regulation of transthyretin in trophoblast biofunction and preeclampsia. *Arch. Biochem. Biophys.* **676**, 108129 (2019).
32. Wu, D., Shi, L., Chen, F., Lin, Q. & Kong, J. Methylation status of the mir-141-3p promoter regulates miR-141-3p Expression, inflammasome formation, and the invasiveness of HTR-8/SVneo cells. *Cytogenet. Genome Res.* **161**(10–11), 501–513 (2021).
33. Ling, Z., Chen, M., Li, T., Qian, Y. & Li, C. MiR-141-3p downregulation promotes tube formation, migration, invasion and inhibits apoptosis in hypoxia-induced human umbilical vein endothelial cells by targeting Notch2. *Reprod. Biol.* **21**(2), 100483 (2021).
34. Zhang, H., Tan, M., Zhang, J., Han, X. & Ma, Y. Propofol Inhibits Thyroid Cancer Cell Proliferation, Migration, and Invasion by Suppressing SHH and PI3K/AKT Signaling Pathways via the miR-141-3p/BRD4 Axis. J Healthc Eng. 2021: 2704753. (2021).
35. Ge, J. et al. SNHG10/miR-141-3p/WTAP axis promotes osteosarcoma proliferation and migration. *J. Biochem. Mol. Toxicol.* **36**(6), e23031 (2022).
36. Ying, H. et al. MiR-127 modulates macrophage polarization and promotes lung inflammation and injury by activating the JNK pathway. *J. Immunol.* **194**(3), 1239–1251 (2015).
37. Köröskényi, K., Kiss, B. & Szondy, Z. Adenosine A2A receptor signaling attenuates LPS-induced pro-inflammatory cytokine formation of mouse macrophages by inducing the expression of DUSP1. *Biochim. Biophys. Acta* **1863**(7 Pt A), 1461–1471 (2016).
38. Wang, Y. et al. Mir-141-5p regulate ATF2 via effecting MAPK1/ERK2 signaling to promote preeclampsia. *Biomed. Pharmacother.* **115**, 108953 (2019).
39. Korkes, H. A. et al. Relationship between hypoxia and downstream pathogenic pathways in preeclampsia. *Hypertens. Pregnancy*. **36**(2), 145–150 (2017).
40. Zhou, X. et al. Impaired placental mitophagy and oxidative stress are associated with dysregulated BNIP3 in preeclampsia. *Sci. Rep.* **11**(1), 20469 (2021).
41. Chen, G. et al. Role of DRAM1 in mitophagy contributes to preeclampsia regulation in mice. *Mol. Med. Rep.* **22**(3), 1847–1858 (2020).
42. Chen, G., Chen, L., Huang, Y., Zhu, X. & Yu, Y. Increased FUN14 domain containing 1 (FUNDC1) ubiquitination level inhibits mitophagy and alleviates the injury in hypoxia-induced trophoblast cells. *Bioengineered*. **13**(2), 3620–3633 (2022).
43. Palikaras, K., Lionaki, E. & Tavernarakis, N. Mechanisms of mitophagy in cellular homeostasis, physiology and pathology. *Nat. Cell. Biol.* **20**(9), 1013–1022 (2018).

Acknowledgements
None.

Author contributions
(I) Conception and design: Dongcai Wu, Humin Gong; (II) Administrative support: Bo Zhou; (III) Provision of study materials or patients: Bo Zhou, Lan Hong; (IV) Collection and assembly of data: Dongcai Wu, Hui Cen, Ling Wang; (V) Data analysis and interpretation: Dongcai Wu, Bo Zhou, Yanlin Ma; (VI) Manuscript writing: Dongcai Wu, Humin Gong; (VII) Final approval of manuscript: All authors.

Funding
This research is granted by National Natural Science Foundation of China (No. 82060285) and Hainan Province Science and Technology Special Fund (ZDYF2022SHFZ120).

Declarations

Consent for publication
Not applicable.

Competing interests
The authors declare no competing interests.

Ethics approval
The animal experiment was approved by the Animal Welfare Committee of Hainan Affiliated Hospital of Hainan Medical University (Med-Eth-Re [2022] 745). We confirm that all methods were reported in accordance with ARRIVE guidelines.

Additional information
Supplementary Information The online version contains supplementary material available at https://doi.org/10.1038/s41598-024-76563-y.

Correspondence and requests for materials should be addressed to H.G.